Talanta 89 (2012) 57–62

Contents lists available at SciVerse ScienceDirect

Talanta

journal homepage: www.elsevier.com/locate/talanta

A novel label-free fluorescent sensor for the detection of potassium ion based on DNAzyme

Xiaoyu Fan, Haitao Li*, Jie Zhao, Fanbo Lin, Lingli Zhang, Youyu Zhang*, Shouzhuo Yao

Key Laboratory of Chemical Biology and Traditional Chinese Medicine Research (Ministry of Education), College of Chemistry and Chemical Engineering, Hunan Normal University, Changsha 410081, PR China

ARTICLE INFO

Article history:
Received 4 September 2011
Received in revised form
16 November 2011
Accepted 20 November 2011
Available online 9 December 2011

Keywords:
Potassium ion
DNAzyme
Fluorescence aptasensor

ABSTRACT

A novel label-free and sensitive fluorescent aptasensor for the detection of potassium ion (K^+) was developed based on the horseradish peroxidase–mimicking DNAzyme (HRP–DNAzyme). In this work, we selected a K^+-stabilized single stranded DNA (ssDNA) with G-rich sequence as the recognition element. In the presence of K^+, the G-rich DNA folded into the G-quadruplex structure, and then hemin can bind to the G-quadruplex structure as a co-factor and form HRP–DNAzyme. 3-(*p*-Hydroxyphenyl)-propanoic acid (HPPA) can be oxidized by H_2O_2 into a fluorescent product in the presence of DNAzyme. The fluorescence intensity of the HPPA oxidative product increased with the K^+ concentration. Under the optimal conditions, the fluorescence intensity was linearly related to the logarithm of K^+ concentration in the range of 2.5 μM to 5 mM. Other metal ions, such as Na^+, Li^+, NH_4^+, Mg^{2+} and Ca^{2+} caused no notable interference on the detection of K^+.

1. Introduction

Potassium ion (K^+) is an important cation in human body. It is essential for preventing muscle contraction and sending of all nerve impulses in animals through action potentials [1]. Normal serum K^+ levels are between 3.8 and 5.4 mmol/L [2]. Abnormal physiological K^+ concentrations may cause several diseases. A severe shortage of potassium in body fluids may cause a potentially fatal condition known as hypokalemia. Excess of K^+ may increase the risk of high blood pressure and stroke [3]. Therefore, the determination of K^+ is very crucial in both clinical diagnosis and basic research. To date, various techniques have been employed to detect K^+ concentration, such as ion chromatography (IC) [2], electrochemistry [3], surface plasmon resonance (SPR) [4], flame atomic absorption spectrometry [5], ion-selective electrodes (ISE) [6] and so on. However, the conventional methods are complex and time-consuming. It is necessary to develop new strategies for K^+ determination. Aptamers are artificial single-stranded oligonucleic acids selected in vitro through systematic evolution of ligands by exponential enrichment (SELEX) [7]. Since the first description in 1990, aptamers have exhibited powerful potential in biochemical analysis field. They have high affinity and selectivity toward a variety of targets, including small molecules [8], proteins [9], metal ions [10], drugs [11], and even whole cells [12]. The appearance of G-quadruplex DNA as a functionalized nucleic acid provides another chance for targets detection. G-quadruplex structure is formed by folding a G-rich random coil single-stranded DNA in the presence of metal ion. A number of sensors have been constructed based on the G-quadruplex [13–17]. Fluorescence measurement is one of the most important analytical techniques. It has played important roles in analytical chemistry, genomics, and biochemical research because of its intrinsic advantages such as high sensitivity, versatility, and low cost [18]. Moreover, G-quadruplex DNA have strong affinity to metal ion, especially K^+, thus, the aptamer sensors combined with fluorescent methods were expected to create a new general platform for biochemical assays based on K^+-stabilized G-quadruplex.

Since standard DNA and RNA aptamers themselves are not inherently fluorescent, most of fluorescent aptamer sensors require an additional modified process. DNA strands labeled with fluorophores were used for the fabrication of these fluorescent aptamer sensors. For example, a K^+ sensor was constructed using a pyrene-labeled molecular beacon as fluorescent probe [19]. He et al., reported a K^+ detection system based on fluorescence resonance energy transfer (FRET) between fluorescein labeled G-quadruplex DNA and water-soluble cationic conjugated polymer (CCP) [20]. However, such labeling strategy bears the drawbacks that the labeling process makes the experiments relatively complex, time-consuming and expensive. More importantly, the labeling with different fluorescent and quenching molecules might affect the original binding affinity and specificity between the aptamers and their targets to some extents, which severely limits the application

* Corresponding authors. Tel.: +86 731 88872046; fax: +86 731 88872046.
E-mail addresses: haitao-li@hunnu.edu.cn (H. Li), zhangyy@hunnu.edu.cn (Y. Zhang).

0039-9140/$ – see front matter © 2011 Elsevier B.V. All rights reserved.
doi:10.1016/j.talanta.2011.11.056

of current aptasensors. Fortunately, using label-free fluorescent method as a technology platform is able to overcome many of these limitations and allow us to realize the label-free target detection. Therefore, a number of G-quadruplex related label-free sensors were developed based on the interaction between G-rich DNA and metal ions. Leung et al., [21] reported a label-free fluorescent detection method for 3′ → 5′ exonuclease activity by using crystal violet as a G-quadruplex binding probe. A series of DNA-related sensors are fabricated based on hemin, G-quadruplex and a newly synthesized anionic conjugated polymer [22].

Because K^+ is of the excellent ability to induce G-rich DNA folding into G-quadruplex, many K^+ sensors were developed based on G-quadruplex [23]. Choi et al., [10] reported a label-free dual assay for DNA and K^+ detection by using $Ru(phen)_2(dppz)^{2+}$ and G-rich DNA. Using an anionic porphyrin protoporphyrin IX (PPIX) as the parallel G-quadruplex-specific fluorescent probe, a fluorescent K^+ monitoring method was described [24]. In this assay, G-rich DNA PS2.M folds into an antiparallel quadruplex structure in sodium-rich solution and it converts into a parallel quadruplex structure while in potassium-rich solution. Because the fluorescent intensity of PPIX can be remarkably enhanced when PPIX binds to the parallel quadruplex structure, the conformational change caused by K^+ is revealed by the distinct enhancement of fluorescent intensity of PPIX. Considering the formation of different G-quadruplex structures under Na^+ or K^+ ion conditions and the ability of crystal violet (CV) to discriminate parallel structures from antiparallel structures of G-quadruplex, Kong et al., [25] developed a fluorescent sensor for monitoring structural changes of G-quadruplex and detecting K^+. Employing the fluorescent dye tetrakis (diisopropylguanidinio) zinc phthalocyanine (Zn-DIGP) as a binding ligand of G-quadruplex, a novel and label-free fluorescent K^+ sensor was developed [1]. Some dyes, such as SYBR Green I (SG) [26] and OliGreen (OG) [27], can intercalate into different DNA structures and result in relative changes of their fluorescent quantum yields. They were also used to design label-free fluorescent sensors to detect K^+. Although a number of G-quadruplex related label-free sensors were developed for the fluorescent determination of potassium ion, it is still essential to improve the sensitivity.

Very recently, on the basis of G-quadruplex, so-called hemin/G-quadruplex horseradish peroxidase–mimicking DNAzyme (HRP–DNAzyme) has attracted considerable interest as a novel biocatalytic label. The single stranded DNA (ssDNA) with G-rich sequence can fold into a more condensed G-quadruplex via intramolecular hydrogen-bonding interaction in the presence of metal ions. The Fe^{3+}-containing porphyrin hemin can intercalate into the G-quadruplex to form HRP–DNAzyme which is able to effectively catalyze the oxidation of 2,2′-azino-bis(3-ethylbenzothiazoline-6-sulfonic acid) ($ABTS^{2-}$) to a colored product [28,29], or the oxidation of luminol to generate chemiluminescence signal [29,30]. Such DNAzymes have been successfully applied to detect metal ions, including K^+ [31], Hg^{2+} [32,33], Ag^+ [34], Pb^{2+} [35], Cu^{2+} [36], UO^{2+} [37] and so on. In Yang's work [38], a DNAzyme-based visible method for K^+ detection are designed based on H_2O_2–3,3′,5,5′-tetramethylbenzidine (TMB) system. In addition, a new label-free fluorescence DNAzyme sensor based on the H_2O_2-mediated oxidation of Amplex UltraRed (AUR) for detecting Pb^{2+} was constructed [39]. In another work, by using 2′,7′-dichlorodihydrofluorescein diacetate (H_2DCFDA) as the reducing substrate, a novel fluorescent analytic approach based on HRP–DNAzyme was developed [40]. Pavlov et al., [41] reported an amplified chemiluminescence detection of DNA and telomerase by using DNAzyme. The Willner's group developed a series of strategies for detecting adenosine monophosphate (AMP) [42,43], protein [43] and DNA [28] by using the HRP–mimicking DNAzyme.

DNAzyme formed from hemin and G-quadruplex has widely attracted attentions because of its excellent catalytic activity similar to HRP. However, most of the reported DNAzyme-based approaches use the DNAzyme as the catalyst for the H_2O_2-mediated oxidation of $ABTS^{2-}$ or luminol and employ colorimetric or chemiluminescence way as the detection method. In fact, label-free K^+ detection with fluorescent method is seldom reported. To our knowledge, there are no previous studies that have reported using such HRP–DNAzyme to design fluorescent sensor for the detection of K^+. 3-(*p*-Hydroxyphenyl)-propanoic acid (HPPA) can be oxidized to a fluorescent product as following equation.

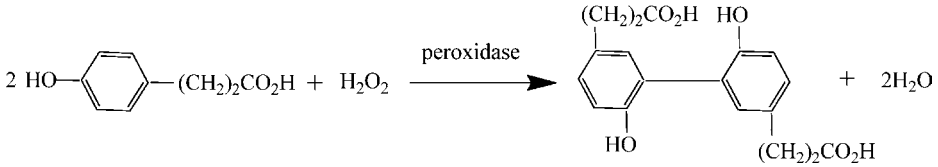

And the reaction can be catalyzed by horseradish peroxidase (HRP), therefore, HRP–DNAzyme can be used to catalyze the oxidation of HPPA with H_2O_2. This work is aimed to develop a simple, sensitive and label-free fluorescent assay for K^+.

2. Experimental

2.1. Oligonucleotide and chemicals

The G-rich oligonucleotide (5′-GTGGGTAGGGCGGGTTGGACCA CACCAACC-3′) used in this study was purchased from Shanghai Sangon Biological Engineering Technology & Services Co., Ltd. The oligonucleotide stoke solution (100 μM) was prepared in Milli-Q ultrapure water (Millipore, ≥18 MΩ cm). Hemin was purchased from TCI (Japan). The stoke solution of hemin (5 mM) was prepared in dimethyl sulfoxide (DMSO) and stored in darkness at −20 °C. HPPA, TMB, H_2O_2 and the used salts such as potassium chloride, sodium chloride, magnesium chloride and calcium chloride were purchased from Shanghai Chemical Reagent Co., Ltd. All chemicals were of analytical grade and used without further purification. The stoke solutions of oligonucleotide and hemin were diluted to the required concentrations with Tris–HCl buffer (10 mM Tris, 100 mM EDTA, pH 8.0) before use. Milli-Qultrapure water was used throughout the experiments.

2.2. Instrumentation

The absorption spectra of hemin, DNAzyme and the oxidative product of TMB were recorded on a UV-2450 spectrophotometer (Shimadzu Co., Japan). An F-4500 fluorescence spectrophotometer (Hitachi Co., Japan) was used to collect the fluorescent emission spectra of the oxidative product of HPPA by H_2O_2.

2.3. Preparation of HRP–DNAzyme

The preparation of HRP–DNAzyme was carried out as described in the literatures [32,34,35,38] with a modified method. Briefly, the oligonucleotide solution containing 16 μM G-rich sequence was heated at 88 °C for 10 min to dissociate any intermolecular

interaction, and then slowly cooled to room temperature. Then, 10 μL of K^+ aqueous solutions of different concentrations were added into 10 μL of the above treated oligonucleotide solutions, respectively and the mixture remained at 25 °C for 40 min in order to form stabilized G-quadruplex structures. After that, the hemin (in DMSO) with a final concentration of 1.8×10^{-5} M was added and incubated in darkness for 2.5 h at 25 °C to form HRP–DNAzyme.

2.4. UV–vis spectroscopic analysis and activity investigation of HRP–DNAzyme

The HRP–DNAzyme prepared according to the above mentioned methods was transferred into quartz cell to collect the Soret band of hemin and DNAzyme (centered at 390–405 nm) with UV-2450 spectrophotometer. Additionally, in order to investigate the activity of the DNAzyme, a TMB–H_2O_2 system was introduced. HRP–DNAzyme solution was added into 100 μL of the enzymatic substrate solution containing 2.08 mM TMB and 4.9 mM H_2O_2, and then the mixture was incubated in darkness at room temperature. After 15 min, the UV–vis spectra of the oxidative product of TMB were recorded.

2.5. Fluorescent determination of potassium ion

The fluorescent measurement for K^+ based on the DNAzyme-catalyzed oxidation of HPPA with H_2O_2 was carried out as follows: 100 μL of the enzymatic substrate solution containing 5×10^{-4} M HPPA and 7.84×10^{-4} M H_2O_2 were mixed with 7 μL of pre-prepared HRP–DNAzyme solution and then kept in darkness for 40 min at 37 °C. After that, fluorescent spectra of the oxidative product of HPPA by H_2O_2 were recorded with excitation wavelength at 320 nm. The fluorescent intensity at 415 nm was used for quantitative analysis of K^+.

3. Results and discussion

3.1. Principle of the potassium ion sensing system

The designed procedure of this DNAzyme-based fluorescent method for K^+ detection was depicted in Fig. 1. In the absence of K^+, the G-rich nucleic acid is in the random coil state. Thus, DNAzyme cannot be formed and the oxidation of HPPA with H_2O_2 cannot be catalytically accelerated. While in the presence of K^+, the G-rich nucleic acid folds into G-quadruplex structure which can bind to hemin to form DNAzyme. The oxidation product was greatly increased with the increasing in DNAzyme concentration. Thus the fluorescence intensity of the oxidative product increases with the increasing in the concentration of K^+.

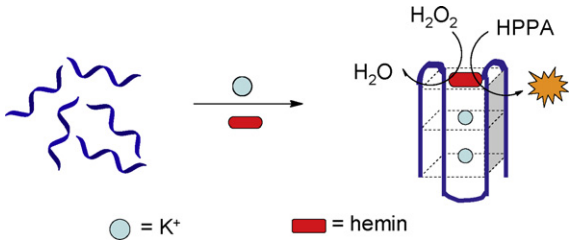

Fig. 1. Proposed scheme for the illustration of the label-free fluorescent aptasensor for detection K^+.

3.2. The formation and activity of HRP–DNAzyme

It is well known that binding of hemin to G-quadruplex is capable of causing distinct hyperchromicity of the hemin's Soret band [32,44–46]. The interactions between hemin and G-rich DNA in the absence and presence of K^+ were investigated by observing the changes of hemin's Soret band in this work. Fig. 2A shows the UV–vis absorption spectra of the solutions of hemin-K^+, hemin–G-rich DNA and hemin-K^+–G-rich DNA. As expected, in the absence of G-rich DNA, a characteristic absorption peak at 397 nm was observed (curve a) for hemin-K^+ solution, which is consistent with the Soret band of the free hemin. For hemin–G-rich DNA, a negligible hyperchromicity in the hemin's Soret band was observed (curve b). But for hemin-K^+–G-rich DNA, an obvious hyperchromicity and red shift of absorption spectrum (7 nm) was observed, suggesting the formation of DNAzyme. These facts showed that hemin can only efficiently interact with G-quadruplex, rather than with G-rich DNA or K^+. It could be concluded that G-rich DNA, K^+ and hemin are essential factors for the formation of DNAzyme.

Fig. 2B shows the UV–vis absorption spectra for different test solutions. The absorption peaks at 370 nm and 652 nm reflect the existence of oxidative product of TMB. Comparing with curve a, a slight absorbance at 370 nm and 652 nm was observed on curve b, which reflects that hemin has weak catalytic activity for the oxidation of TMB with H_2O_2. Much greater absorbance was recorded for curve c, indicating that the oxidation of TMB with H_2O_2 was greatly accelerated by DNAzyme. Accordingly, a noticeable color change of the solution was observed while DNAzyme was added suggesting that the DNAzyme has the HRP-like catalytic activity toward the oxidation of TMB with H_2O_2.

3.3. Optimization of the DNAzyme formation condition

The formation of G-quadruplex-hemin DNAzyme is closely related with various factors such as temperature, pH, and incubation time. In order to obtain a high-sensitive sensor for the

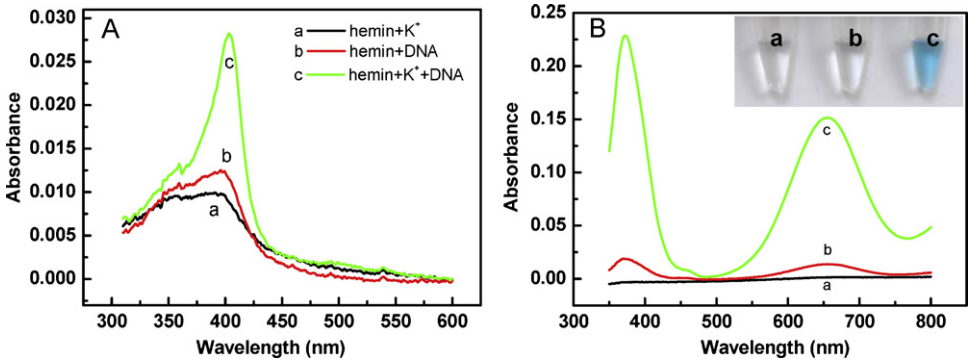

Fig. 2. (A) UV–vis spectra of 1.8×10^{-5} M hemin in pH 8.0 Tris–HCl buffer in the absence and presence of K^+ or G-rich DNA. (a) incubation with 5 mM K^+; (b) incubation with 8 μM G-rich DNA; (c) incubation with 5 mM K^+ and 8 μM G-rich DNA. (B) UV–vis spectra of TMB solution in pH 5.0 HAc–NaAc buffer, (a) after reaction with H_2O_2; (b) reaction with H_2O_2 catalyzed by hemin; (c) reaction with H_2O_2 catalyzed by DNAzyme, respectively. The inset was the photographed images of the reaction solution.

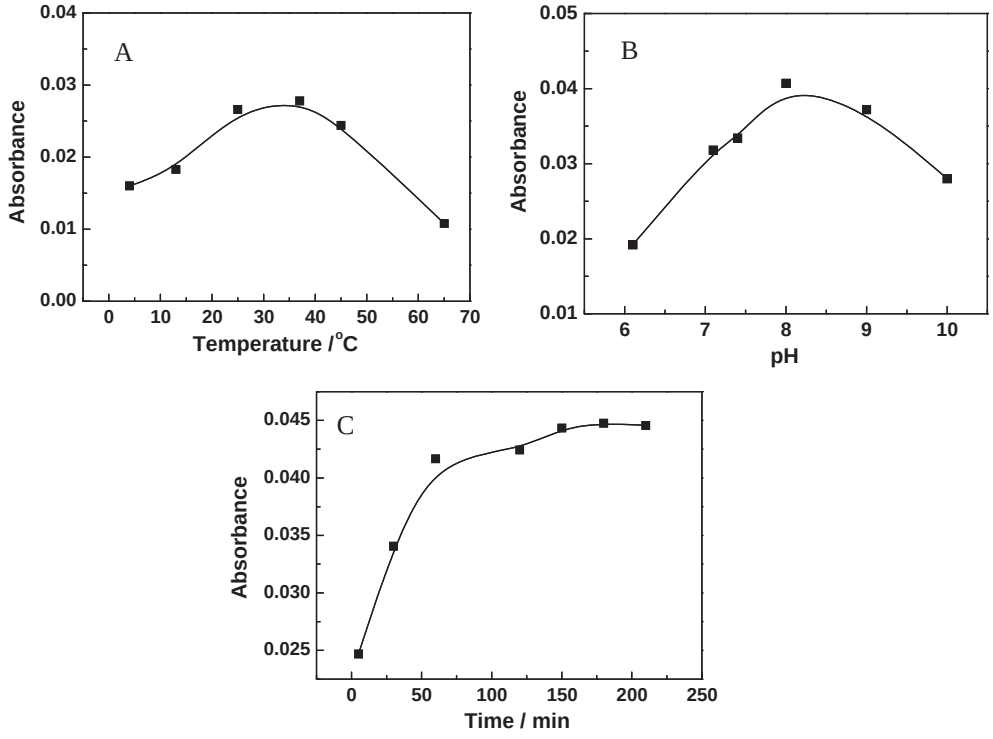

Fig. 3. The UV–vis absorbance of the resulted DNAzyme at various incubation temperature in Tris–HCl (pH 8.0) for 150 min (A), with different pH values at 25 °C for 150 min (B), for various incubation time in Tris–HCl (pH 8.0) at 25 °C (C). Other experimental conditions were the same as those described in Fig. 2A curve c. $\lambda_{Abs(max)}$ = 404 nm.

detection of K^+, the optimization of the conditions for DNAzyme formation is essential. Firstly, the effect of incubation temperature in the range from 4 °C to 65 °C on the formation of DNAzyme was investigated. As shown in Fig. 3A, the UV–vis absorption intensity related to the formation of DNAzyme increased with the rising of the incubation temperature in the range of 4–37 °C, but it declined when the incubation temperature was higher than 37 °C. These phenomena are possibly related to the formation of K^+-stabilized G-quadruplex structure and the activity of hemin. Previous literatures [47] reported that low temperature is in favor of forming the G-quadruplex. When the temperature is higher than 37 °C, the G-quadruplex became unstable and could be easily destructed to single-stranded DNA. Considering hemin might hold higher activity in the physiological conditions, the most favorable incubation temperature to form DNAzyme should be around 37 °C. Since only a small difference in absorption intensity was observed between the test solutions incubated at 25 °C and 37 °C, respectively, 25 °C (room temperature) was used as the incubation temperature in our experiments.

Since the configuration of DNA would be greatly affected by pH value, the effect of buffer pH on the formation of DNAzyme was investigated in this work. As shown in Fig. 3B, the absorption related to the formation of DNAzyme increased with increasing pH value and reached the maximum value at pH 8.0. When the pH was further increased, the absorption intensity decreased. This phenomenon is probably attributed to the increased negative charges of DNA molecules which led to the disintegration of G-quadruplex when pH > 8.0 [48]. The result was in conformity with the previous related reports [32,38]. Thus, Tris–HCl buffer (pH 8.0) was selected as the working buffer in the following experiments.

The effect of the incubation time on the performance of the sensor was also investigated. Fig. 3C shows the time-dependent absorbance response of DNAzyme. We can see that the absorbance signal at 404 nm sharply increased with increasing the incubation time from 5 min to 60 min and then enhanced gradually and tended to level off after 150 min. It is suggested that the interaction of hemin with G-quadruplex reached equilibrium within 150 min. Therefore, 150 min was employed as the proper incubation time.

3.4. Optimization of the catalytic reaction conditions for the fluorescence detection

In addition to the formation of DNAzyme catalyst, the catalytic reaction condition for the oxidation of HPPA with H_2O_2 also has very important impacts on the detection. Thus, it is necessary to optimize the relevant experiment variables, such as the catalytic reaction time, temperature, concentrations of HPPA and H_2O_2. The experimental results are presented in Fig. 4. As shown in Fig. 4A, the measured fluorescence intensity increased with the increasing in H_2O_2 concentration in the range of 0.2–0.8 mM and then declined at higher H_2O_2 concentration. The appearance of the maximum fluorescence intensity implies that the catalytic activity of the DNAzyme reaches the top stage at the vicinity of 0.8 mM H_2O_2 and excess of H_2O_2 would decline the catalytic ability of the DNAzyme. Hence, 0.784 mM H_2O_2 was adopted for the subsequent assays.

The effect of HPPA concentration was investigated and the results are shown in Fig. 4B. When HPPA concentration was lower than 0.5 mM, the fluorescence intensity increased rapidly with the increasing in HPPA concentration. While HPPA concentration was higher than 0.5 mM, the fluoresce responses reduced with the increasing in HPPA concentration. It has been reported that phenols can be oxidized in the presence of hydrogen peroxide and generated radicals which react with aromatic substances to form dimeric, oligomeric, or polymeric by-products [49]. Therefore, we presumed that the decrease in the fluorescence intensity may be attributed to the generation of other HPPA oxidative products resulted from the higher concentration of HPPA. Consequently, 0.5 mM of HPPA was employed as the optimal concentration for the test systems.

Fig. 4C illustrates the effect of the time on the catalytic reaction. The fluorescence intensity quickly increased with the increasing in

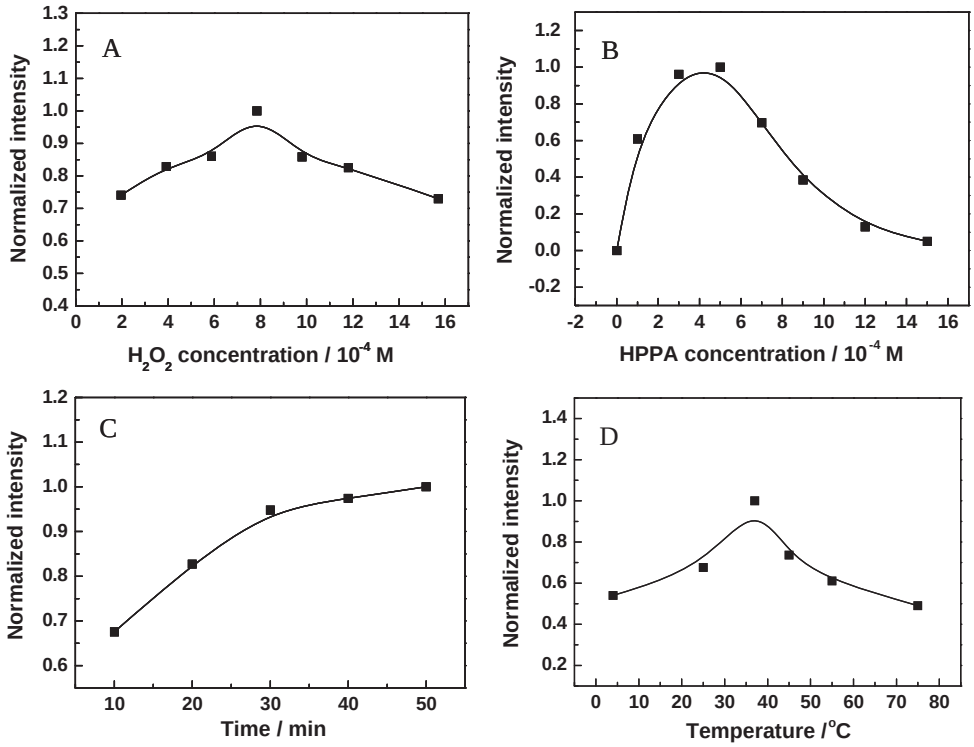

Fig. 4. The fluorescent response of the oxidation product of HPPA with H_2O_2 catalyzed by DNAzyme in Tris–HCl solutions (pH 8.0) (A) containing 5×10^{-4} M HPPA and different concentrations of H_2O_2 at 37 °C for 40 min; (B) containing 7.84×10^{-4} M H_2O_2 and different concentrations of HPPA at 37 °C for 40 min; (C) containing 7.84×10^{-4} M H_2O_2 and 5×10^{-4} M HPPA for various catalytic reaction time at 37 °C;(D) containing 7.84×10^{-4} M H_2O_2 and 5×10^{-4} M HPPA at various catalytic reaction temperature for 40 min. λ_{em} = 415 nm.

reaction time and reached an equilibrium value for about 40 min. Therefore, the catalytic reaction was conducted for 40 min in our subsequent experiments. Fig. 4D depicts the fluorescent response of the sensor at various catalytic reaction temperatures of 4 °C, 25 °C, 37 °C, 45 °C, 55 °C and 75 °C. It was observed that the fluorescent signal rose rapidly as the reaction temperature increased from 4 °C to 37 °C, and then decreased gradually at higher temperature than 37 °C. As demonstrated in Section 3.3, the temperature can seriously affect the catalytic activity of DNAzyme via destroying its structure. This temperature dependence of the fluorescent signal is consistent with that of DNAzyme catalytic activity. Therefore, the physiological temperature of 37 °C was chosen as the optimum catalytic reaction temperature.

3.5. The analytical performance of the sensor

The analytical performances of the sensor for the detection of K^+ were investigated under the optimum experimental conditions. The fluorescence intensity of the oxidative product emission spectra maximum increased with the K^+ concentration (Fig. 5). A linear relationship between the fluorescence intensity and the logarithm of K^+ concentration ranging from 2.5 μM to 5 mM was obtained. The linear regression equation was $F = 0.10085 \log C + 1.19588$ with a linear correlation coefficient of 0.9723, where F refers to the measured fluorescence intensity and C refers to the concentration of K^+. These experimental results demonstrated that the proposed method for K^+ detection is comparable with other reported methods (Table S1, Supporting information).

In order to evaluate the selectivity of the proposed sensor for the detection of K^+, comparative trials were carried out by using Na^+, Li^+, NH_4^+, Ca^{2+} or Mg^{2+} as the potential interference ions. Fig. 6 shows the changes in the fluorescence intensity of the sensor with the addition of different cations. The results show that only K^+ caused a marked response on the fluorescent intensity at 415 nm and other metal ions has no obvious interference, suggesting that this proposed sensing system is specific for the detection of K^+.

3.6. Application of the sensor

The sensor was further applied to perform K^+ assay for a real blood serums sample. The serum sample was diluted 100-fold and added into different amount of K^+ solution. The resultant mixtures were tested following the proposed strategy to record

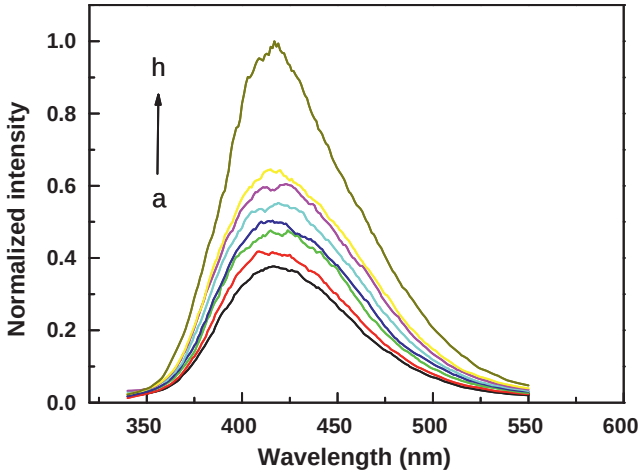

Fig. 5. Fluorescent response of the oxidative product of HPPA upon addition of different concentrations of K^+: (a) 0 μM, (b) 2.5 μM, (c) 25 μM, (d) 250 μM, (e) 350 μM, (f) 2.5 mM, (g) 5 mM, (h) 25 mM in the DNAzyme–HPPA–H_2O_2 system. Experiment conditions: 10 mM Tris–HCl buffer of pH 8.0 containing 7.84×10^{-4} M H_2O_2 and 5×10^{-4} M HPPA.

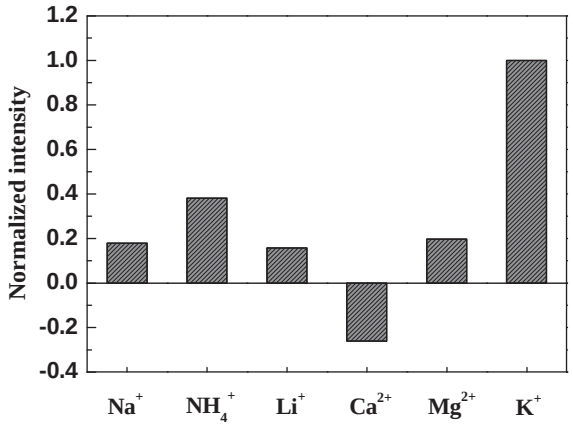

Fig. 6. Specificity of K^+ assay against other metal ions. Na^+, Li^+, NH_4^+, Mg^{2+}, Ca^{2+} and K^+ were used at the same concentration of 2.5 mM. Other experiment conditions were the same as those described in Fig. 5. The fluorescent response of K^+ was defined as 1.

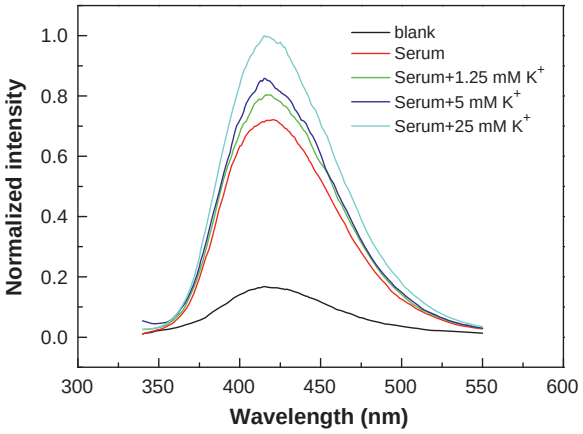

Fig. 7. Fluorescent response of the oxidative product of HPPA upon the addition of Tris–HCl buffer, blood serum and blood serum mixed with different concentrations of K^+. Other experiment conditions were the same as those described in Fig. 5.

the fluorescence response. The results are shown in Fig. 7, which showed that the fluorescence intensity of the reaction mixture increased upon the increased concentration of the added K^+. The experimental results suggested that the sensor can be used to detect the K^+ in real samples.

4. Conclusions

In summary, a novel label-free fluorescent aptasensor for the determination of K^+ was developed, using horseradish peroxidase-mimicking DNAzyme as the catalyst for the oxidation of HPPA with H_2O_2. A linear response to logarithm of K^+ concentration in the range from 2.5 μM to 5 mM was obtained. The assay method exhibits a good selectivity for K^+ over other metal ions. Compared with previous reports about the detection of K^+, the proposed strategy is label-free, simple, specific, and sensitive. More importantly, it is the first and successful attempt to detect K^+ with a fluorescence method based on the catalytic activity of HRP–DNAzyme in the H_2O_2-mediated oxidation of HPPA. We believe that the present reported DNAzyme biosensor will provide a versatile tool for the determination of K^+ in wide areas.

Acknowledgment

This work was supported by the National Natural Science Foundation of China (20975037, 21075037), and Scientific Research Fund of Hunan Provincial Science and Technology Departments (09JJ3019, 07JJ3024), and Aid program for Science and Technology Innovative Research Team in Higher Educational Instituions of Hunan Province.

Appendix A. Supplementary data

Supplementary data associated with this article can be found, in the online version, at doi:10.1016/j.talanta.2011.11.056.

References

[1] H. Qin, J. Ren, J. Wang, N.W. Luedtke, E. Wang, Anal. Chem. 82 (2010) 8356–8360.
[2] B. Yu, L. Nie, S. Yao, J. Chromatogr. B 693 (1997) 43–49.
[3] M.F.S. Teixeira, B.H. Freitas, P.M. Seraphim, L.O. Salmazo, M.A. Nobre, S. Lanfredi, Proc. Chem. 1 (2009) 293–296.
[4] H. Chen, Y.S. Gal, S.H. Kim, H.J. Choi, M.C. Oh, J. Lee, K. Koh, Sens. Actuators B: Chem. 133 (2008) 577–581.
[5] A.d. Jesus, M.M. Silva, M.G.R. Vale, Talanta 74 (2008) 1378–1384.
[6] S. Kim, H. Kim, K.H. Noh, S.H. Lee, S.K. Kim, J.S. Kim, Talanta 61 (2003) 709–716.
[7] C. Tuerk, L. Gold, Science 249 (1990) 505–510.
[8] C. Deng, J. Chen, L. Nie, Z. Nie, S. Yao, Anal. Chem. 81 (2009) 9972–9978.
[9] H. Chang, L. Tang, Y. Wang, J. Jiang, J. Li, Anal. Chem. 82 (2010) 2341–2346.
[10] M.S. Choi, M. Yoon, J.O. Baeg, J. Kim, Chem. Commun. (2009) 7419–7421.
[11] C. Zhang, L.W. Johnson, Anal. Chem. 81 (2009) 3051–3055.
[12] Y. Wang, Z. Li, D. Hu, C.-T. Lin, J. Li, Y. Lin, J. Am. Chem. Soc. 132 (2010) 9274–9276.
[13] E. Sharon, R. Freeman, I. Willner, Anal. Chem. 82 (2010) 7073–7077.
[14] K. Meguellati, G. Koripelly, S. Ladame, Angew. Chem. Int. Ed. 49 (2010) 2738–2742.
[15] K. Zhang, X. Zhu, J. Wang, L. Xu, G. Li, Anal. Chem. 82 (2010) 3207–3211.
[16] Y. Lin, C. Liu, H. Chang, Talanta 84 (2011) 324–329.
[17] W. Cai, Y. Fan, Z. Jiang, J. Yao, Talanta 81 (2010) 1810–1815.
[18] Y. Xiang, Z. Wang, H. Xing, N.Y. Wong, Y. Lu, Anal. Chem. 82 (2010) 4122–4129.
[19] C. Shi, H. Gu, C. Ma, Anal. Biochem. 400 (2010) 99–102.
[20] F. He, Y. Tang, S. Wang, Y. Li, D. Zhu, J. Am. Chem. Soc. 127 (2005) 12343–12346.
[21] C. Leung, D.S. Chan, B.Y. Man, C. Wang, W. Lam, Y. Cheng, W. Fong, W.W. Hsiao, D. Ma, Anal. Chem. 83 (2011) 463–466.
[22] B. Li, C. Qin, T. Li, L. Wang, S. Dong, Anal. Chem. 81 (2009) 3544–3550.
[23] D.-M. Kong, J.-H. Guo, W. Yang, Y.-E. Ma, H.-X. Shen, Biosens. Bioelectron. 25 (2009) 88–93.
[24] T. Li, E. Wang, S. Dong, Anal. Chem. 82 (2010) 7576–7580.
[25] D. Kong, Y. Ma, J. Guo, W. Yang, H. Shen, Anal. Chem. 81 (2009) 2678–2684.
[26] H. Xu, S. Gao, Q. Yang, D. Pan, L. Wang, C. Fan, ACS Appl. Mater. Interfaces 2 (2010) 3211–3216.
[27] C. Huang, H. Chang, Chem. Commun. (2008) 1461–1463.
[28] Y. Xiao, V. Pavlov, T. Niazov, A. Dishon, M. Kotler, I. Willner, J. Am. Chem. Soc. 126 (2004) 7430–7431.
[29] J. Li, Q. Yao, H. Fu, X. Zhang, H. Yang, Talanta 85 (2011) 91–96.
[30] Y. Weizmann, Z. Cheglakov, I. Willner, J. Am. Chem. Soc. 130 (2008) 17224–17225.
[31] T. Li, E. Wang, S. Dong, Chem. Commun. (2009) 580–582.
[32] T. Li, S. Dong, E. Wang, Anal. Chem. 81 (2009) 2144–2149.
[33] D. Kong, J. Wu, N. Wang, W. Yang, H. Shen, Talanta 80 (2009) 459–465.
[34] X. Zhou, D. Kong, H. Shen, Anal. Chem. 82 (2010) 789–793.
[35] T. Li, E. Wang, S. Dong, Anal. Chem. 82 (2010) 1515–1520.
[36] B. Yin, B. Ye, W. Tan, H. Wang, C. Xie, J. Am. Chem. Soc. 131 (2009) 14624–14625.
[37] M. Moshe, J. Elbaz, I. Willner, Nano Lett. 9 (2009) 1196–1200.
[38] X. Yang, T. Li, B. Li, E. Wang, Analyst 135 (2010) 71–75.
[39] C. Li, K. Liu, Y. Lin, H. Chang, Anal. Chem. 83 (2011) 225–230.
[40] B. Qiu, Z. Zheng, Y. Lu, Z. Lin, K. Wong, G. Chen, Chem. Commun. 47 (2011) 1437–1439.
[41] V. Pavlov, Y. Xiao, R. Gill, A. Dishon, M. Kotler, I. Willner, Anal. Chem. 76 (2004) 2152–2156.
[42] G. Pelossof, R. Tel-Vered, J. Elbaz, I. Willner, Anal. Chem. 82 (2010) 4396–4402.
[43] C. Teller, S. Shimron, I. Willner, Anal. Chem. 81 (2009) 9114–9119.
[44] P. Travascio, A.J. Bennet, D.Y. Wang, D. Sen, Chem. Biol. 6 (1999) 779–787.
[45] M. Wang, Y. Han, Z. Nie, C. Lei, Y. Huang, M. Guo, S. Yao, Biosens. Bioelectron. 26 (2010) 523–529.
[46] P. Travascio, Y. Li, D. Sen, Chem. Biol. 5 (1998) 505–517.
[47] J. Zhao, Y. Zhang, H. Li, Y. Wen, X. Fan, F. Lin, L. Tan, S. Yao, Biosens. Bioelectron. 26 (2011) 2297–2303.
[48] J. Zhang, Y. Wang, Y. He, T. Jiang, H. Yang, X. Tan, R. Kang, Y. Yuan, L. Shi, Anal. Biochem. 397 (2010) 212–217.
[49] A. Wilkens, J. Paulsen, V. Wray, P. Winterhalter, J. Agric. Food Chem. 58 (2010) 6754–6761.